

# INVESTIGATING SELECTIVE REMOVAL OF Cr(VI) AND ZINC IONS FROM AQUEOUS MEDIA BY MECHANICAL-CHEMICAL ACTIVATED RED MUD

N. Ghanbarpouraboli, Sh. Raygan\* and H. Abdizadeh

\* shraygan@ut.ac.ir

Received: February 2016

Accepted: November 2016

School of Metallurgy and Materials Engineering, College of Engineering, University of Tehran, Tehran, Iran.

**Abstract:** In this study, the adsorption of hexavalent chromium and zinc ions from the solution is investigated by raw red mud and mechanical-chemical activated red mud along with the possibility of selective reclamation of these ions from the solution. The mechanical-chemical activation of red mud was done by employing high-energy milling and subsequent acid treatment with  $\text{HNO}_3$ . Raw red mud (RRM) and mechanical-chemical activated red mud (MCARM) adsorbents were characterized with Fourier transform infrared spectroscopy (FTIR), X-ray fluorescence (XRF), X-ray diffraction (XRD), scanning electron microscope (SEM), and Brunauer–Emmett–Teller (BET) methods. In order to determine the suitable adsorption conditions, effects of pH of the solution, amount of adsorption, temperature, and time of adsorption were investigated. It was found that the optimum pH for the adsorption of hexavalent chromium and zinc ions by MCARM adsorbent was 2 and 6, respectively. According to these pH values, MCARM had the ability to separately adsorb more than 95 and 79% of hexavalent chromium and zinc ions from the solution, respectively. Experimental results were in good agreement with Langmuir and Freundlich isotherms. By considering the kinetic models of adsorption, the kinetics of the adsorption of both ions followed the pseudo-second-order reaction model. It was also determined that almost 25.8 and 61.8% of the hexavalent chromium and zinc ions adsorbed in MCARM could be recovered.

**Keywords:** Red Mud, Mechanical-chemical Activation, Hexavalent Chromium, Zinc, Kinetics, Isotherms, Adsorption, Desorption.

## 1. INTRODUCTION

Recently, due to the restriction of safe water supplies and increasing water pollution caused by industries, serious concerns about the protection of safe water sources have been aroused. One of the most deteriorative water polluting agents is heavy metals, which can be a serious harm for the environment and humans due to the high environmental stability and severe toxicity [1-3]. The presence of heavy metals in industrial wastewater, which are produced in metallurgical industries, mining activities, painting, and coating production centers, in addition to the possible contamination of water sources can pollute soil [4-6]. Among the heavy metals, hexavalent chromium and zinc ions exist in different industrial wastewaters [7, 8]. Meanwhile, World Health Organization (WHO) has determined the maximum allowance concentration of hexavalent chromium and zinc ions for drinking water as 0.1 and 5 ppm, respectively [9-10].

Various methods for the purification of

wastewater containing heavy metals have been developed and used, among which are chemical precipitation, ion exchange, membrane filtration, coagulation and flocculation, and adsorption. Most of these methods either are expensive or have low efficiency [11]. The purification of wastewater by the surface adsorption of inexpensive adsorbents due to low cost, high efficiency, and easy operational applications has attracted the attention of many researchers [12]. In this procedure, by processing the organic or mineral industrial waste, adsorbents with high absorption ability of heavy metals from the solute are produced.

Red mud is an industrial waste of the Bayer process in the alumina production and annually millions of tons of it are produced. This material is stored in tailing dams and/or throws in the seas, which creates many environmental problems [13]. In the recent years, many investigations have been conducted in order to use red mud for different applications, especially as an inexpensive adsorption for the removal of heavy metals from solutions [13]. Because of the

presence of metal oxides such as  $\text{Al}_2\text{O}_3$ ,  $\text{Fe}_2\text{O}_3$ ,  $\text{TiO}_2$ , and tiny particles in red mud, it can be used as an adsorbent. However, raw red mud has a high alkaline characteristic ( $\text{pH} > 12$ ) and needs an activation step in order to be prepared for surface adsorption [14].

The aim of this investigation is to study the possibility of selective removal of hexavalent chromium and zinc ions, which are simultaneously present in the solution by raw red mud (RRM) or mechanical-chemical activated red mud (MCARM). The effects of different parameters on determining proper conditions such as pH, time, temperature, and adsorbent content as well as thermodynamics and kinetics of adsorption are studied. Recovery of the adsorbed ions is also investigated.

## 2. EXPERIMENTAL PROCEDURE

### 2. 1. Materials

The raw red mud used in this research was obtained from Iran Alumina Company. All the materials including  $\text{K}_2\text{Cr}_2\text{O}_7$  (No.1.04864.0500),  $\text{ZnCl}_2$  (No.1.08816.0250),  $\text{HNO}_3$  (No.1.00443.2500),  $\text{NaOH}$  (No.1.06462.1000), and  $\text{NH}_4\text{OH}$  (No. 1.05426.2500) were with analytical grade and obtained from Merck (Germany). In order to prepare the stock solution containing hexavalent chromium and zinc ions, 266.2 and 669.1 g of  $\text{K}_2\text{Cr}_2\text{O}_7$  and  $\text{ZnCl}_2$  were weighted and dissolved in 2 l of deionized water to produce a solution with 400 ( $\text{mg l}^{-1}$ ) concentration of hexavalent chromium and zinc ions.

### 2. 2. Activation of Red Mud

After washing with deionized water, the red mud was dried at  $60^\circ\text{C}$  within 24 h. In order for the mechanical activation, the raw red mud was milled for 5 h by a planetary mill (Asia-Sanat-Rakhsh- PM2400) at room temperature using hardened stainless steel vials (hardness of 60 HRC) and balls (hardness of 55 HRC) which were resistant to corrosion and wear. Three different ball diameters of 5, 10 and 12 mm with equivalent weight were utilized. The ball to

powder mass ratio and rotation speed of vial were 15:1 and 200 rpm, respectively. Then, the mechanically activated red mud was acid treated with 1 N nitric acid in 1 h. Subsequently, the solution was neutralized by ammonia solution 25% and pH was adjusted to 7. After the filtration, the adsorbent was washed twice with deionized water and dried at  $60^\circ\text{C}$  within 24 h.

### 2. 3. Adsorbent Characterization

The RRM and MCARM powders were analyzed by X-ray diffraction (XRD) using  $\text{CuK}\alpha$  radiation ( $\lambda = 1.5455 \text{ \AA}$ ) at 30 kV and tube current of 30 mA over the  $2\theta$  range from 20 to 90 degrees and Fourier transform infrared spectroscopy (FTIR), Nicolat IR 100, in the range of 400-4000 ( $\text{cm}^{-1}$ ). X-ray fluorescence (XRF), Philips wp1480, was used to identify the chemical composition of the samples. The morphology of the samples was examined by scanning electronic microscope (SEM), LEO1400. The specific area of the adsorbents was measured by Brunauer–Emmett–Teller (BET) method using nitrogen gas. Particle size distribution was analyzed by a wet particle size analyzer manufactured by Fritsch GmbH.

### 2. 4. Absorption and Recovery Tests

All the experiments were performed by batch technique in the solutions containing hexavalent chromium and zinc ions with the volume of 50 (ml) simultaneously. The solutions with different concentrations were prepared by the dilution of stock solution with deionized water. Different amounts of RRM and MCARM adsorbents were weighted and added to the test solutions for adsorbing the hexavalent chromium and zinc ions. Then, they were stirred by a magnetic stirrer at the approximate speed of 400 rpm. The pH of the solution was measured by a pH meter, (BellPHS3-BW), and adjusted by 0.1 molar sodium hydroxide and 0.1 molar nitric acid solutions. After performing the adsorption tests and for separating the adsorbents from the solutions, they were centrifuged at the speed of 5000 rpm for 2 min (SIGMA2-16KCH) and filtered by Whatman42 filter paper. The

remaining solution was analyzed by inductively coupled plasma (ICP) method (Varian LIBERTY-RL) to determine the hexavalent chromium and zinc ion concentration. The percentage of removed ions (R) and the amount of adsorbate in the adsorbent at equilibrium ( $q_e$ ) were calculated by Eqs. 1 and 2, respectively [15].

$$R(\%) = (C_0 - C_f) / C_0 \times 100 \quad (1)$$

$$q_e = [(C_0 - C_f) \times V] / m \quad (2)$$

where  $C_0$  and  $C_f$  are, respectively, the initial and final concentrations of ions in the solution ( $\text{mg l}^{-1}$ ),  $V$  is volume of solution (l), and  $m$  is adsorbent mass (g).

The MCARM with the highest absorption amount was selected for the recovery tests of adsorbed ions. In this regard, adsorption process was done by mixing MCARM with 200 ml solution and contact time of 20 min. The concentration of each Chromium and Zinc ions in this solution was  $400 \text{ mg l}^{-1}$ . In order to recover the ions, 4.8 g of the above mentioned MCARM was

added to 100 ml of deionized water. Recovery tests were done at two pH levels of 2 and 6, separately. pH of the solution was adjusted by  $\text{NH}_4\text{OH}$  25% and 0.5 M  $\text{HNO}_3$ . The solution was stirred for 1 h at the speed of 400 rpm at room temperature.

### 3. RESULTS AND DISCUSSION

#### 3. 1. RRM and MCARM Characterization

Figure 1 shows diffraction patterns of RRM and MCARM sample, which confirms the presence of hematite ( $\text{Fe}_2\text{O}_3$ ), cancrinite ( $\text{Na}_8(\text{Al}_6\text{Si}_6\text{O}_{24})(\text{OH})_{2.04}(\text{H}_2\text{O})_{2.66}$ ), vaterite ( $\text{CaCO}_3$ ), quartz ( $\text{SiO}_2$ ), calcium titanium oxide ( $\text{CaTiO}_3$ ), and anatase ( $\text{TiO}_2$ ) phases in RRM. Diffraction pattern of MCARM adsorbent shows only the hematite phase. The inability to identify some other phases in the MCARM in comparison with the RRM can be ascribed to the existence of residual stress in the crystal lattice structure because of milling stage. This issue leads to some changes in lattice parameter and formation of

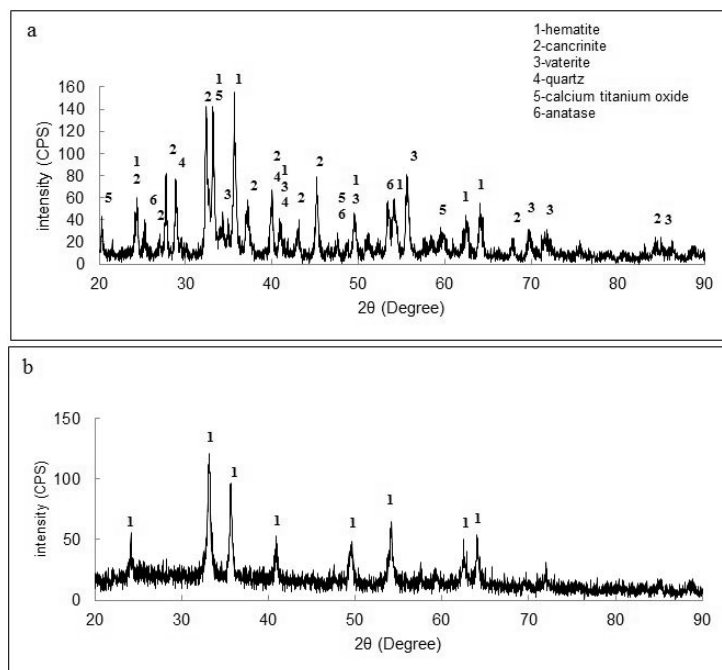


Fig. 1. XRD pattern of (a) RRM and (b) MCARM.

Table 1. Chemical composition of RRM and MCARM

Component	RRM	MCARM
	Constituent%	
Fe <sub>2</sub> O <sub>3</sub>	23.74	39.87
Al <sub>2</sub> O <sub>3</sub>	19.24	10.39
CaO	19.91	8.75
SiO <sub>2</sub>	16.13	14.67
TiO <sub>2</sub>	12.96	17.32
Na <sub>2</sub> O	4.56	2.11
MgO	0.24	0.14
ZrO <sub>2</sub>	0.19	0.21
K <sub>2</sub> O	0.18	0.12
Loss of ignition	2.85	6.42

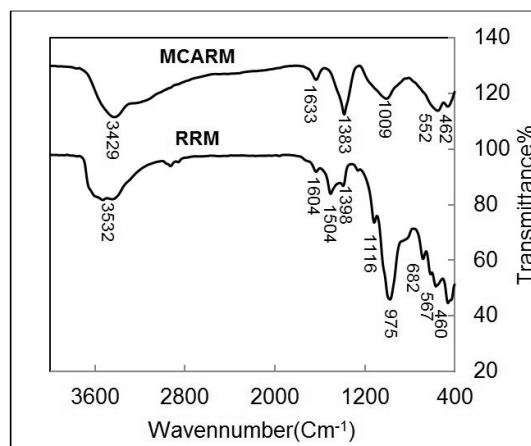


Fig. 2. FTIR spectra of RRM and MCARM.

amorphous compounds. Some of the components could be also removed during chemical activation and the acid treatment stage after mechanical milling.

The chemical composition of the RRM and MCARM adsorbents was determined by XRF method and the results are listed in Table 1.

The results showed that, after the mechanical-chemical activation of red mud, the percentage of iron and titanium oxides was increased. However, the percentage of calcium, aluminum, and silicon oxides decreased during the activation processes. Figure 2 shows the FTIR spectra of RRM and MCARM adsorbents. The peak bonds at 460 and 567 cm<sup>-1</sup> in the RRM sample and 462 and 552 cm<sup>-1</sup> in the MCARM sample can be related to the stretching vibrations of Fe-O bonds and stretching the Al-O-Si bonds, respectively. In addition, the peak in the wave number of 682 cm<sup>-1</sup> corresponded to the Ti-O bond. The 1398 and 1504 cm<sup>-1</sup> peaks in the RRM sample were matched with the stretching vibrations of C=O bonds, which was due to the presence of the carbonate compounds in the sample. In the RRM and MCARM samples, the peaks at the 1604 and 1633 cm<sup>-1</sup> were related to the vibration of the H-O-H bonds, which confirmed the presence of H<sub>2</sub>O molecules in the structure of both adsorbents. H-O bond can be also detected in the wave number of 3532 and 3429 cm<sup>-1</sup>. The

vibration of Si-O bond in the RRM at the wave number of the 975 and 1116 cm<sup>-1</sup> and in the MCARM at the wave number of 1009 cm<sup>-1</sup> was also observed. In the case of MCARM sample, the strong peak at 1383 was detected, which was associated with the N=O bond [16, 17]. The existence of the N=O bond might be related to the formation of ammonium nitrate in the chemical activation process, according to reaction 3.



The specific surface area of RRM and MCARM adsorbents was 14 m<sup>2</sup>g<sup>-1</sup> and 176 m<sup>2</sup>g<sup>-1</sup>, respectively. Figure 3 depicts the distribution of particle size for two studied adsorbents. The results demonstrated that, due to the mechanical-chemical activation, the average size of red mud particles decreased from 56.28 to 3.83 μm, which was one of the most important reasons for increasing the specific surface area of MCARM sample.

The SEM images of RRM and MCARM adsorbents are shown in Figure 4. It can be observed that the MCARM adsorbent had smaller particle size than the RRM adsorbent. Due to the reduction in red mud particle sizes and a significant increase in specific surface area as a result of the chemical-mechanical activation, MCARM adsorbent can be expected to have

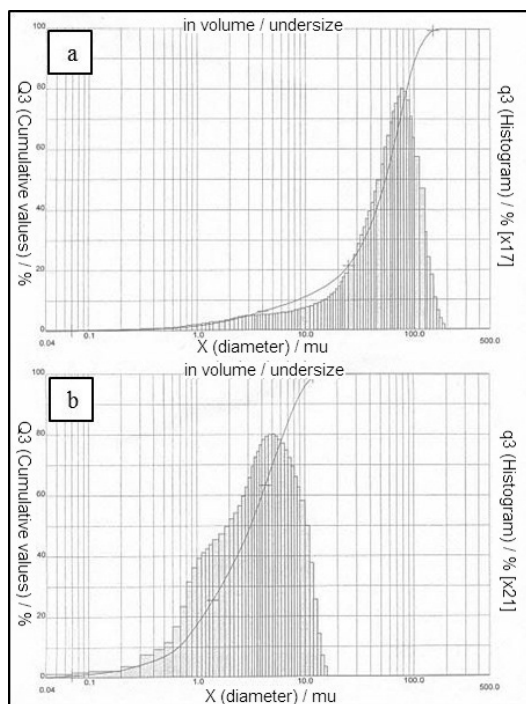


Fig. 3. Particle size distribution of (a) RRM and (b) MCARM.

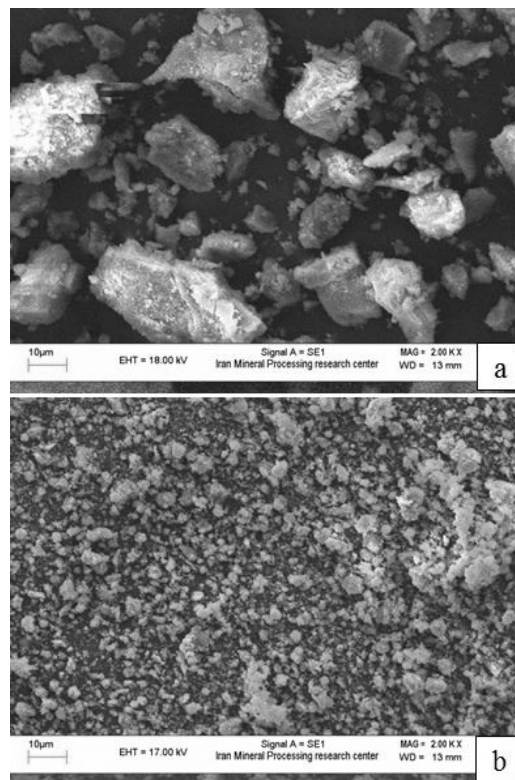


Fig. 4. SEM micrograph of (a) RRM and (b) MCARM.

much better adsorption capability than RRM.

### 3. 2. Effect of pH

In this study, the effect of initial pH of the solution on the adsorption of Cr(VI) and Zn ions was studied using RRM and MCARM adsorbents in the pH range of 1.5 to 12. pH is one of the main surface adsorption parameters, which affects adsorbent surface charge and ionic species of adsorbate [18]. The experiments were done on the solution containing 25 mg<sup>l</sup>-<sup>1</sup>Cr(VI) and Zn ions during the 30 min stabilization period at room temperature with 2 g of adsorbent. Figure 5 shows the simultaneous chromium and zinc ions removal by RRM adsorbent. By increasing the pH value, at first, the percentage of Cr(VI) ion removal slightly increased and, then, decreased. Regarding the Zn ion, with increasing the pH value up to 7, a minor increase in the adsorption of Zn could be observed. However, at the pH of greater than 7, the adsorption increased

significantly, which was not related to the Zn ion adsorption by the adsorbent. This phenomenon was related to the precipitation of insoluble zinc hydroxide in the solution [19,20].

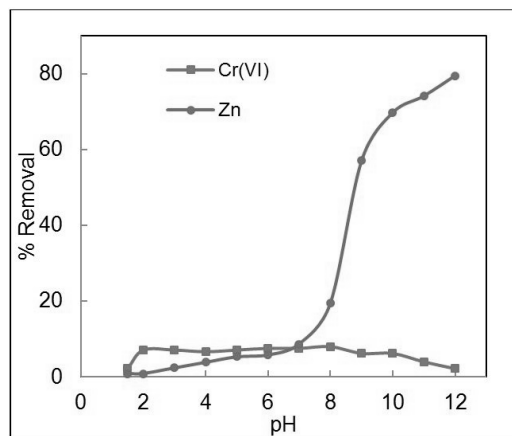


Fig. 5. Effect of initial pH on the removal of Cr(VI) and Zn ions by RRM.

Figure 6 illustrates simultaneous Cr(VI) and Zn ions removal by MCARM adsorbent. The adsorption of Cr(VI) ion in the pH range of 2 to 8 was almost constant and more than 95 percent of Cr(VI) was removed by MCARM. In this case, the maximum value of removal (98%) occurred at the pH of 2. Nevertheless, at the pH of greater than 8, the removal of Cr(VI) ion was reduced and, finally, at the pH of 12, it reached 72%. At the pH of 1.5, a significant decrease in the adsorption of Cr(VI) ion by the adsorbent was observed, which could be related to the partial dissolution of red mud at this pH. The adsorption amount of Zn ions at the pH of 1.5 was 4.8%. With increasing pH up to 3, no considerable change was observed in adsorption. However, at the pH of greater than 3, the ion removal was increased gradually and reached 79%. At the pH of greater than 7, at first, the removal percentage was constant and, then, increased again, which could occur due to the hydroxide precipitation [19, 20].

The adsorption of ions on the surface of an adsorbent can be explained by the particle surface charge. The surface charge of the adsorbent particles was strongly affected by the pH of the solution. In this case, the  $pH_{PZC}$  parameter was defined, which was actually the pH at which the adsorbent surface charge was zero. In the pH values of less than  $pH_{PZC}$ , due to the protonation

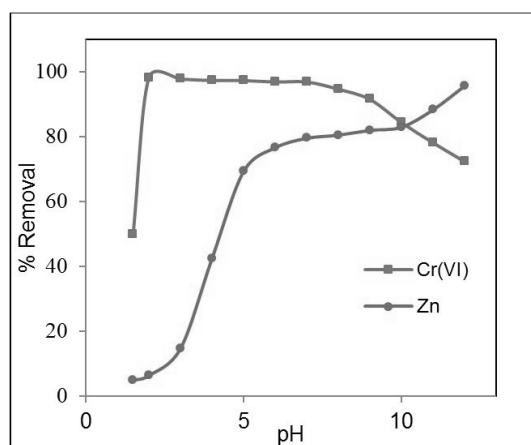
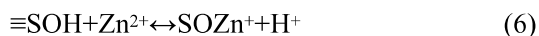


Fig. 6. Effect of initial pH on removal of Cr(VI) and Zn ions by MCARM.

of functional group (OH), the surface charge became positive. At the pH values of higher than  $pH_{PZC}$ , because of the functional group (OH) deprotonation, the surface charge became negative. The charge of surface particles created a bond between the adsorbents and the adsorbates [21]. The  $pH_{PZC}$  of the red mud surface should be locally considered. It means that, according to the pH values, every component on the red mud surface can be positive or negative and, consequently, based on hexavalent chromium anion or zinc cation, it could be adsorbed. The ionic species of hexavalent chromium in the pH range of 2 to 5 was in the form of  $HCrO_4^-$  and, at the higher pH value, the  $CrO_4^{2-}$  anion was gradually stabilized [22]. All of the components in the activated red mud, in the strong acidic pH, had a positive surface charge and an ability to adsorb the chromium ions [23]. The adsorption of chromium ion at the pH of higher than 8 can be decreased due to the presence of  $CrO_4^{2-}$  ions which, in comparison with the  $HCrO_4^-$ , had a greater negative charge and also increased the surface charge of red mud with pH. In addition, at  $pH > 7$ , there was a competition between  $OH^-$  and  $CrO_4^{2-}$  ions for being adsorbed by the adsorbent surface [12]. Zinc at  $pH < 7$  was just in the form of  $Zn^{+2}$  and zinc hydroxide was gradually formed at  $pH > 7$  [24]. The  $pH_{PZC}$  of silicon and titanium oxides was about 3; this parameter was about 7.5 for iron and aluminum oxides [23]. Therefore, silicon and titanium oxides at the pH of greater than 3 had a negative surface charge and can adsorb zinc cation. Thus, adsorption of zinc ion increased with the pH of greater than 3. According to the surface complex model, Cr(VI) anions and Zn cations with the hydroxyl group on the surface can create a bond. Eqs. 4 to 7 illustrate the bond between the Cr(VI) and Zn ions with the surface. In these equations, S is the symbol of adsorbent hydroxylated surface. Each of the iron, silicon, titanium, and aluminum oxides can create a hydroxyl group on the surface [22, 26].





### 3. 3. Effect of Adsorbent

In these experiments, at first, 50 ml solution with the concentration of 25 mg<sup>-1</sup>Cr(VI) and Zn ions was prepared and its pH was adjusted to 2 by adding 1.0 M acid nitric for adsorbing Cr(VI) by various amounts of RRM and MCARM adsorbents. Subsequently, the separation of the solution from the adsorbent was done by a filter paper and the pH of the solution was adjusted to 6 with 1.0 M sodium hydroxide solution. Then, by adding fresh adsorbent to the almost free Cr(VI) solution, the adsorption of zinc ion was studied by various amounts of RRM and MCARM adsorbents. Figure 7 indicates the variation in the removal of Cr(VI) and Zn ions against the amount of RRM and MCARM adsorbents. It can be seen that the absorption of Cr(VI) and Zn ions slightly increased with the increment of the amount of RRM adsorbent. In contrast, with increasing the amount of MCARM adsorbent, the adsorption of Cr(VI) and Zn ions was increased considerably. This phenomenon can be related to the possible enhancement of absorption sites as a result of increasing the amount of adsorbent. It can be observed that less

than 10% of Cr(VI) and Zn ions was removed by RRM adsorbent. However, this amount was more than 95% for Cr(VI) and 80% for Zn ions by MCARM adsorbent.

### 3. 4. Adsorption Isotherms

Adsorption isotherms are used for determining the adsorption capacity of the adsorbent material and expressing the equilibrium state of adsorbate and adsorbent. In order to determine the adsorptive capacity of MCARM, some experiments were done at different concentrations of Cr(VI) and Zn ions from 25 to 400 mg<sup>-1</sup> and with 1.2 g of the adsorbent.

Langmuir isotherm has been proposed for adsorbing a monolayer of adsorbate on the homogeneous surfaces. The following equation is the linear form of the Langmuir isotherm [27]:

$$C_e/q_e=1/bQ_m+C_e/Q_m \quad (8)$$

In this equation,  $q_e$  and  $Q_m$  are equilibrium adsorption capacity and maximum adsorption capacity (mgg<sup>-1</sup>), respectively.  $C_e$  is the equilibrium concentration of the adsorbate (mg<sup>-1</sup>) and  $b$  is the Langmuir isotherm constant (lm<sup>-1</sup> g<sup>-1</sup>). Figure 8 shows the linear form of the Langmuir isotherm of Cr(VI) ion adsorption at pH=2 and the Zn ion adsorption at pH=6. The high values of

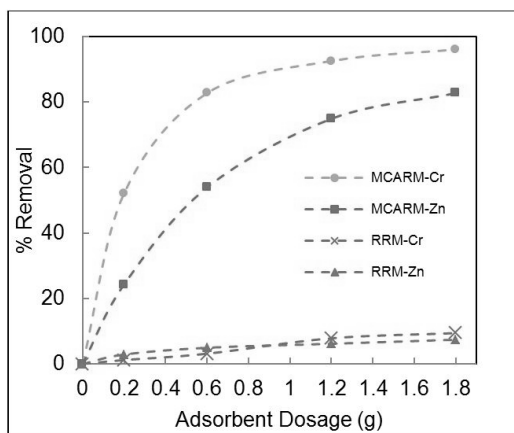


Fig. 7. Effect of RRM and MCARM dosage on Cr(VI) and Zn removal.

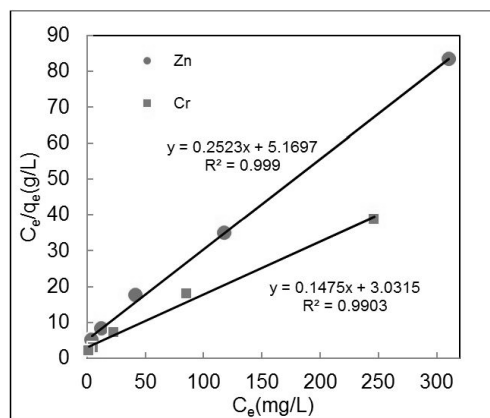


Fig. 8. Langmuir isotherm for adsorption of Cr(VI) and Zn ions by MCARM.

**Table 2.** Langmuir and Freundlich isotherm parameters for the adsorption of Cr(VI) at pH= 2 and Zn at pH=6 by MCARM at different concentrations

ion	pH	Langmuir isotherm			Freundlich isotherm		
		$Q_m(\frac{mg}{g})$	$b(\frac{L}{mg})$	$R^2$	$K_F$	N	$R^2$
Cr <sup>6+</sup>	2	6.7	0.048	0.99	0.87	2.6	0.97
Zn <sup>2+</sup>	6	3.9	0.048	0.99	0.58	2.8	0.95

correlation coefficient demonstrate the high agreements of the experimental results with Langmuir model. Therefore, it can be expressed that the adsorption of chromium and zinc by MCARM surface might be monolayer.

Maximum calculated adsorption capacity of Cr(VI) and Zn ions was 6.7 and 3.9 mgg<sup>-1</sup>), respectively. The Freundlich isotherm has been

also proposed for adsorption on heterogeneous surfaces. Eq. 9 shows the linear form of Freundlich isotherm [28]:

$$\text{Log}q_e = \text{Log}K_f + 1/n \text{Log}C_e \quad (9)$$

where  $q_e$  and  $C_e$  are equilibrium adsorption capacity (mgg<sup>-1</sup>) and the equilibrium

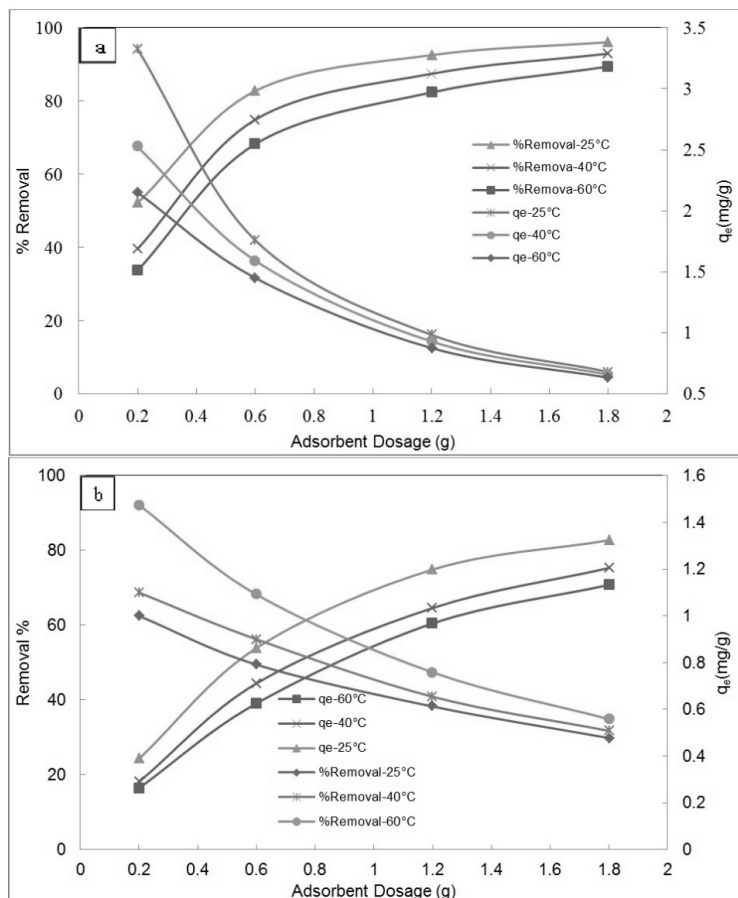


**Fig. 9.** Effect of temperature on adsorption capacity and removal percent of (a) Cr(VI) (b) Zn ions by MCARM.

concentration of adsorbate ( $\text{mg l}^{-1}$ ), respectively.  $n$  and  $KF$  are the Freundlich isotherm parameters, which are tabulated in Table 2.

Correlation coefficient values showed that Freundlich isotherm can be also applied for the adsorption of  $\text{Cr(VI)}$  and  $\text{Zn}$  ions by MCARM adsorbent.

### 3. 5. Effect of Temperature

To investigate the effect of temperature on the absorption of  $\text{Cr(VI)}$  and  $\text{Zn}$  ions by MCARM adsorbent and also study the thermodynamic of adsorption for these two ions, adsorption experiments with the initial concentration of  $25 \text{ mg l}^{-1}$  for each ion and different amounts of MCARM adsorbent at 25, 40, and  $60^\circ\text{C}$  were performed. The effect of temperature on the  $\text{Cr(VI)}$  and  $\text{Zn}$  ions uptake is drawn in Figure 9.

By using the Langmuir isotherm (Figure 10), the maximum adsorption capacity at different temperatures was calculated and presented in Table 3. It is seen that the maximum adsorption capacity for  $\text{Cr(VI)}$  ion was decreased from 5.45 to 4.15 by the increment of the temperature from 25 to  $60^\circ\text{C}$ . This reduction in adsorption amount for  $\text{Zn}$  ion was from 2.80 to 2.31. In other words, the capability of MCARM adsorbent in removing  $\text{Cr(VI)}$  and  $\text{Zn}$  ions was decreased with increasing temperature, which emphasized the exothermic nature of the adsorption process by MCARM adsorbent.

By considering Eqs. 10 to 13 and the Langmuir isotherm, the thermodynamic parameters such as Gibbs free energy ( $\Delta G^\circ$ ), standard enthalpy

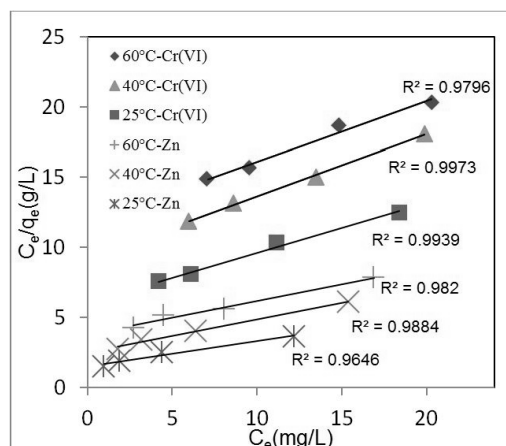


Fig. 10. Langmuir plot of  $\text{Cr(VI)}$  and  $\text{Zn}$  ions adsorption by MCARM at different temperatures.

( $\Delta H^\circ$ ), and standard entropy ( $\Delta S^\circ$ ) of  $\text{Cr(VI)}$  and  $\text{Zn}$  ions adsorption by MCARM adsorbent can be calculated [29].

$$\Delta G^\circ = \Delta H^\circ - T\Delta S^\circ \quad (10)$$

$$\Delta G^\circ = -RT \ln K \quad (11)$$

$$K = b \times M_A \quad (12)$$

$$\ln K = \Delta S^\circ / R - \Delta H^\circ / RT \quad (13)$$

where  $b$  is the Langmuir isotherm constant,  $M_A$  is molar mass of adsorbate,  $R$  is gas universal constant, and  $T$  is temperature. By plotting the variation of  $\ln(K)$  against  $1/T$  (Eq.12), the

Table 3. Thermodynamic parameters for the adsorption of  $\text{Cr(VI)}$  and  $\text{Zn}$  ions by MCARM

Ion	pH	$Q_m$	Temperature (K)	Thermodynamic parameters		
				$\Delta G^\circ (\text{kJ mol}^{-1})$	$\Delta H^\circ (\text{kJ mol}^{-1})$	$\Delta S^\circ (\text{kJ mol}^{-1} \text{K}^{-1})$
$\text{Cr}^{6+}$	2	5.45	298	-4.61	-15.37	-0.0361
	2	4.24	313	-4.07		
	2	4.15	333	-3.34		
$\text{Zn}^{2+}$	6	2.80	298	-3.36	-11.39	-0.0269
	6	2.24	313	-2.96		
	6	2.31	333	-2.42		

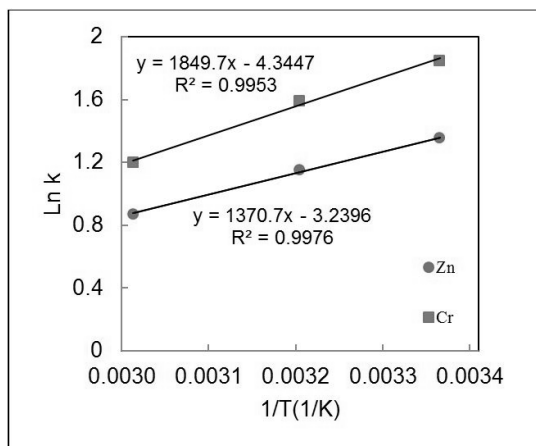


Fig. 11. Arrhenius plot for Cr(VI) and Zn ions adsorption by MCARM.

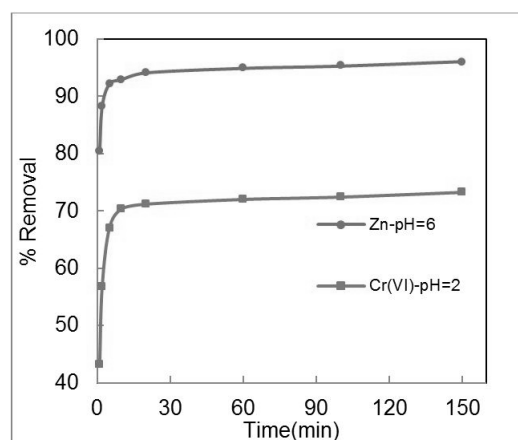


Fig. 12. Effect of time on the Cr(VI) and Zn ions adsorption by MCARM.

thermodynamic parameters of adsorption can be calculated (Figure 11). The thermodynamic parameters of adsorption for Cr(VI) and Zn ions are listed in Table 3. The negative values of  $\Delta G$  for Cr(VI) and Zn by MCARM adsorbent illustrate that the adsorption process for both ions was spontaneous.

### 3. 6. Effect of Time

The adsorption of Cr(VI) and Zn ions by MCARM adsorbent at different times was studied in order to determine the adsorption equilibrium time and adsorption kinetic model. Adsorption experiments with 1.2 g of MCARM adsorbent were performed at room temperature. The corresponding results are shown in Figure 12. It is clear that the adsorption of Cr(VI) and Zn ions by MCARM adsorbent took approximately 20 min to reach its equilibrium value. In order to determine the kinetic of adsorption, pseudo- first-

order model, pseudo-second-order model, and intra-particle diffusion model were considered.

The models for pseudo-first-order, pseudo-second-order, and intra-particle diffusion models are described by Eqs. 14, 15, and 16, respectively [30].

$$\text{Log}(q_e - q_t) = \text{Log} q_e - k_1 t / 2.303 \quad (14)$$

$$t/q_t = 1/K_2 q_e^2 + t/q_e \quad (15)$$

$$\text{Log} q_t = \text{Log} K_{id} + a \text{Log} t \quad (16)$$

In these equations,  $q_t$  and  $q_e$  are adsorption capacity at time  $t$  and adsorption capacity in the equilibrium state ( $\text{mg g}^{-1}$ ), respectively. Also,  $K_1$  and  $K_2$  are the rate constant of the pseudo-first-order adsorption ( $\text{min}^{-1}$ ) and rate constant of pseudo-second-order adsorption ( $\text{g mg}^{-1} \text{min}^{-1}$ ), respectively.  $K_{id}$  and  $a$  are the intra-particle diffusion rate constant and empirical constant,

Table 4. Kinetic parameters for the adsorption of Cr(VI) and Zn ions by MCARM

Ion	pH	Pseudo first-order kinetic			Pseudo second-order kinetic			Intraparticle diffusion		
		$k_1$	$q_e$	$R^2$	$k_2$	$q_e$	$R^2$	$k_{id}$	$a$	$R^2$
$\text{Cr}^{6+}$	2	0.0005	0.39	0.361	2.95	1.02	0.999	0.904	0.024	0.747
$\text{Zn}^{2+}$	6	0.0027	0.07	0.475	2.08	0.74	0.999	0.527	0.082	0.6848

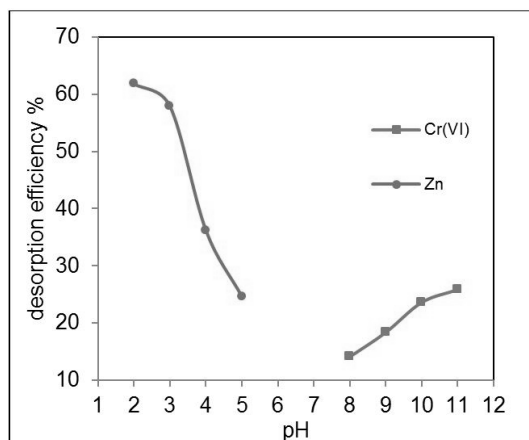


Fig. 13. Desorption of Cr(VI) and Zn ions from MCARM with respect to solution pH.

respectively. The parameters of model and their correlation factors are summarized in Table 4. The high values of correlation factor,  $R^2$ , show that the adsorption of Cr(VI) and Zn ions by MCARM adsorbent is followed by the pseudo-second-order reaction.

### 3. 7. Recovery of Ions from Adsorbent

Recovery of the adsorbed Cr(VI) ions from the MCARM adsorbent was studied at the pH of 8, 9, 10, and 10.5. Also, the pH levels of 2, 3, 4, and 5 were selected for the recovery of adsorbed zinc ion from MCARM adsorbent. Figure 13 shows the results of these tests. Maximum recovery of zinc ion was 61.8% at the pH of 2 and, by increasing pH, it was strongly decreased and reached 24.6% at the pH of 5. The recovery rate of Cr(VI) ion at pH=8 was 14.1% which increased gradually with the increment of pH and, finally, reached 25.8% at the pH of 10.5. The lower recovery rate in Cr(VI) ion can be ascribed to the stronger bond between chromium ion and adsorbent surface.

## 4. CONCLUSIONS

In this study, the adsorption of hexavalent chromium and zinc ions from the solution by raw red mud (RRM) and mechanical-chemical activated red mud (MCARM) as well as the

possibility of separating these ions from each other was investigated. The results showed that:

The specific area of the red mud was increased from 14 to 176  $\text{m}^2 \text{g}^{-1}$  due to the mechanical-chemical activation process. As a result, the capability of the red mud for ion adsorption was significantly increased. MCARM adsorbent could adsorb 95% of Cr(VI) ion at the pH of 2 and 79% zinc ion at the pH of 6. Accordingly, chromium and zinc ions could be separately adsorbed on the surface of MCARM. Langmuir isotherm matched the results of adsorption of both Cr(VI) and zinc ions by MCARM well. The absorptive capacity of the Cr(VI) ion by MCARM adsorbent and zinc ion was 5.45  $\text{mgg}^{-1}$  and 2.80  $\text{mgg}^{-1}$ , respectively. Using the Langmuir isotherm and thermodynamic equations,  $\Delta G$  for Cr(VI) and zinc ions were calculated at 4.61 and 3.36  $\text{kJmol}^{-1}$ , respectively. The kinetics of adsorption was relatively fast and, after 20 min, the adsorbent and adsorbate reached the equilibrium. The recovery of zinc ion from loaded MCARM (61.8%) was much greater than that of Cr(VI) ion (25.8%).

## REFERENCES

- Jiang, M. Q., Jin, X. Y., Lu, X. Q. and Chen, Z. L., "Adsorption of Pb(II), Cd(II), Ni(II) and Cu(II) onto Natural Kaolinite Clay. Desalination". 2010, 252, 33-39.
- Polat, H. and Erdogan, D., "Heavy metal Removal From Waste Waters by Ion Flotation". J. Hazard. Mater. 2007,148, 267-273.
- Abo-Farha, S. A., Abdel-Aal, A. Y., Ashour, I. A. and Garamon, S. E., "Removal of Some Heavy Metal Cations by Synthetic Resin Purolite C100. J. Hazard. Mater. 2009,169, 190-194.
- Jusoh, A., Shiung, L. S., Ali, N. and Noor, M. J. M. M., "A Simulation Study of the Removal Efficiency of Granular Activated Carbon on Cadmium and Lead". Desalination. 2007, 206, 9-16.
- Kaczala, F., Marques, M. and Hogland, W., "Lead and Vanadium Removal From a Real Industrial Wastewater by Gravitational Settling/Sedimentation and Sorption onto Pinussylvestris Sawdust". Bioresource.

- Technol. 2009, 100, 235-243.
6. Wang, Z., Liu, G., Fan, Z., Yang, X., Wang, J. and Wang, S., "Experimental Study on Treatment of Electroplating Wastewater by Nanofiltration". *J. Membrane. Sci.* 2007, 305, 185-195.
  7. Pillaya, K., Cukrowska, E. M. and Coville, N. J., "Multi-walled Carbon Nanotubes as Adsorbents for the Removal of Parts Per Billion Levels of Hexavalent Chromium from aqueous solution". *J. Hazard. Mater.* 2009, 166, 1067-1075.
  8. Ahu, R. C., Patel, R. and Ray, B. C., "Adsorption of Zn(II) on activated red mud: Neutralized by CO<sub>2</sub>". *Desalination.* 2011, 266, , 93-97.
  9. Sen, T. K. and Gomez, D., "Adsorption of zinc (Zn<sup>2+</sup>) from aqueous Solution on Natural Bentonite". *Desalination.* 2011, 267, 286-294.
  10. Nataraj, S. K., Hosamani, K. M. and Aminabhavi, T. M., "Potential Application of an Electrodialysis Pilot Plant Containing Ion-Exchange Membranes in Chromium Removal". *Desalination.* 2007, 217, 181-190.
  11. Fu, F. and Wang, Q., "Removal of Heavy Metal Ions From Wastewaters": A Review. *J. Environ. Manage.* 2011, 92, 407-418.
  12. Pradhan, J., Das S. N. and Thakur R. S., "Adsorption of Hexavalent Chromium From Aqueous Solution by Using Activated Red Mud". *J. Colloid. Interf. Sci.* 1999, 217, 137-141.
  13. Wang, S., Ang, H. M. and Tade, M. O., "Novel Applications of Red Mud as Coagulant, Adsorbent and Catalyst for Environmentally Benign Processes". *Chemosphere.* 2008, 72, 1621-1635.
  14. Sushil, S. and Batra, V. S., "Catalytic Applications of Red Mud", an Aluminium Industry Waste: A Review. *Appl. Catal. B-Environ.* 2008, 81, 64.
  15. Liu, Q. S., Zheng, T., Wang, P., Jiang, J. P. and Li, N., "Adsorption Isotherm, Kinetic and Mechanism Studies of Some Substituted Phenols on Activated Carbon Fibers". *Chem. Eng. J.*, 2010, 157, 348-356.
  16. Stuart, B. H., "Infrared Spectroscopy: Fundamentals and Applications", John Wiley & Sons Ltd, 2004, 95-110.
  17. Socrates, G., "Infrared and Raman Characteristic Group Frequencies": Tables and Charts, John Wiley & Sons Ltd, 2001.
  18. Altundogan, H. S., Altundogan, S., Tumen, F. and Bildik, M., "Arsenic Removal From Aqueous Solutions by Adsorption on Red Mud. *Waste Manage.* 2000, 20, 761-767.
  19. Ding, P., Huang, K. L., Li, G. Y., Liu, Y. F. and Zeng, W. W., "Kinetics of Adsorption of Zn(II) Ion on Chitosan Derivatives". *Inter. J. Biol. Macromol.* 2006, 39, 222-227.
  20. Malamis, S. and Katsou, E., "A Review on Zinc and Nickel Adsorption on Natural and Modified Zeolite", Bentonite and Vermiculite: Examination of Process Parameters, Kinetics and Isotherms. *J. Hazard. Mater.* 2013, 252-253, 428-461.
  21. Mamindy-Pajany, Y., Hurel C., Marmier, N. and Romeo, M., "Arsenic Adsorption onto Hematite and Goethite". *CR Chim.* 2009, 12, 876-881.
  22. Erdem, M., Altundoagan, H. S. and Tumen, F., "Removal of Hexavalent Chromium by Using Heat-Activated Bauxite". *Miner. Eng.* 2004, 17, 1045-1052.
  23. Wasewar, K. L., Atif, M., Prasad, B. and Mishra, I. M., "Batch Adsorption of Zinc on Tea Factory Waste", *Desalination.* 2009, 244,, 66-71.
  24. Kosmulski, M., "PH-Dependent Surface Charging and Points of Zero Charge". IV. Update and New Approach. *J. Colloid Inter. Sci.* 2009, 337, 439-448.
  25. Phan, T. N. T., Louvard, N., Bachirib, S. A., Persello, J. and Foissy, A., "Adsorption of Zinc on Colloidal Silica", Triple Layer Modelization and Aggregation Data. *Colloids Surf. A.* 2004. 244, 131-140.
  26. Luo, L., Ma, C., Ma, Y., Zhang, S., Lv, J. and Cui, M., "Newlinsights into the Sorption Mechanism of Cadmium on Red Mud". *Environ. Pollut.* 2011, 159, 1108-1113.
  27. Bubba, M. D., Arias, C. A. and Brix, H., "Phosphorus Adsorption Maximum of Sands for Use as Media in Subsurface Flow Constructed Reed Beds as Measured by the Langmuir Isotherm". *Water Resour.* 2003, 37, 3390-3400.
  28. Ng, C., Losso J. N., Marshall W. E. and Rao R. M., "Freundlich Adsorption Isotherms of

- Agricultural By-Product-Based Powdered Activated Carbons in a Geosmin–Water System”. *Bioresour. Technol.* 2002, 85, 131-135.
29. Liu, Y., “Some Consideration on the Langmuir Isotherm Equation. *Colloids Surf*”. A., 2006, 274, 34-36.
  30. Gurses, A., Dogar, C., Yalcın, M., Acıkyıldız, M., Bayrak, R. and Karaca, S., “The Adsorption Kinetics of the Cationic Dye”, Methylene Blue, onto Clay. *J. Hazard. Mater.* 2006, B131, 217-228.